COMPRESSIVE STRENGTH OF A CARBON FIBER IN MATRIX

M. Ueda[1*], A. Hiraga[2], T. Nishimura[1]
[1] College of Science & Technology, Nihon University, Tokyo, Japan
[2] Graduate School of Nihon University, Tokyo, Japan
* Corresponding author (ueda@mech.cst.nihon-u.ac.jp)

Keywords: *Carbon fiber, Compression, micro-buckling, kink-band*

1 Introduction

Tensile strength of the unidirectional carbon fiber reinforced plastic (CFRP) has been increasing with increase of tensile strength of the reinforcing carbon fiber. On the other hand, compressive strength of the CFRP has not been increased. Compressive strength of unidirectional CFRP is about 50 to 60% of its tensile strength [1, 2]. Since CFRP is used for beam structures of aircraft which carry bending moment, it may fail at compression side prior to the tensile side. Compressive strength is, therefore, a design criterion of the CFRP structure. Compressive strength of the CFRP should be improved to increase structural reliability and reduce more weight of aircraft structures.

There are many reports on the compressive strength of CFRP [3-16]. Representative compression failure is micro-buckling of fibers [3-5]. Prediction of compressive strength was based on the kink-band model [6-10] or the column buckling on elastic foundation model [11-16].

The former model predicts compressive strength using macroscopic properties of the CFRP. It is, therefore, difficult to indicate dominant factors to prevent fiber micro-buckling (kink band failure).

The latter model predicts compressive strength from the microscopic properties of the CFRP. Compressive strength is predicted from the fiber, matrix and interfacial properties. Although there are some reports on the prediction of compressive strength of unidirectional CFRP by the model of column buckling on elastic foundation [14-16] it has not been validated for the prediction of compressive strength of a single fiber in matrix. It is also important to meaure compressive strength of a carbon fiber to improve compressive strength of the CFRP. However, compressive strength of a carbon fiber is not fully understood yet because it is difficult to test [17-20].

In this study, compressive strength of a carbon fiber in epoxy matrix is predicted based on a model of column buckling on elastic foundation in which fiber misalignment, matrix nonlinearity and fiber bending is taken into considered. The relationship between kink-band model and column buckling on elastic foundation model is discussed. Analytical results are compared to experimental results from which compressive strength of a carbon fiber is discussed.

2 Buckling stress of a single fiber in matrix

Fig. 1 shows a single fiber in an infinite matrix. The fiber buckles in the matrix due to applied axial load. The matrix supports the fiber elastically until its yield. The fiber buckles in the x-y plane.

Two patterns of fiber buckling deformation were supposed. Fig. 2(a) shows bending deformation. This deformation is supposed to occur for a single fiber in matrix (in the case of low fiber volume fraction). Fig. 2(b) shows shear deformation. This deformation supposed to occur for a unidirectional CFRP in which kink band failure is observed as a compressive failure (in the case of high fiber volume fraction) [3-5].

An infinitesimal element taken from the fiber is shown in Fig. 3. P_f, Q_f and M_f are axial compressive force, shearing force and bending moment. q is lateral force per unit length by elastic foundation. v is deflection of the fiber. It is supposed that fiber has initial misalignment v_0 and no deformation is developed during the fabrication of the composite.

From the infinitesimal element of the fiber, resulting equation of equilibrium is

$$\frac{d^2 M_f}{dx^2} - P_f \frac{d^2 v}{dx^2} - q = 0 \tag{1}$$

In the case of bending deformation (Fig. 2a) bending moment can be written as

$$M_f = -E_f I_f \frac{d^2 (v - v_0)}{dx^2} \tag{2}$$

Where E_f is Young's modulus of fiber and I_f is moment of inertia of fiber.

In the case of shear deformation (Fig. 2b) bending moment can be written as

$$M_f = \frac{\pi d_f^{\,2}}{4} \int G_f \frac{d(v - v_0)}{dx} dx \tag{3}$$

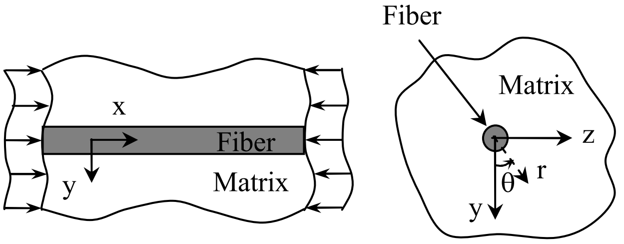

Fig. 1 A single fiber in infinite matrix under uniaxial compression

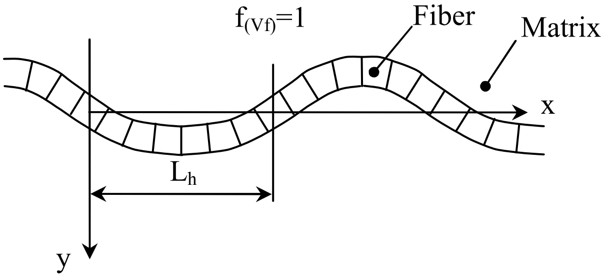

(a) Buckling of a single fiber
(In case of low fiber volume fraction)

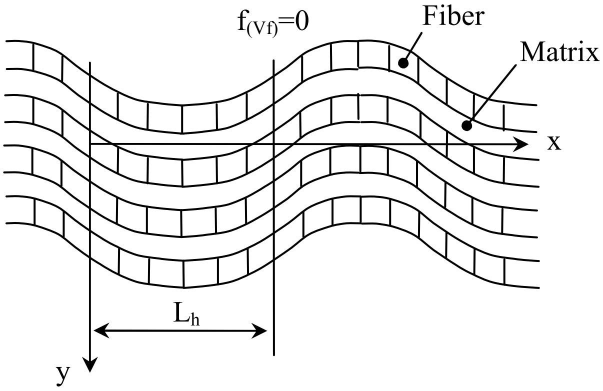

(b) In-phase buckling of fibers
(In case of high fiber volume fraction)
Fig. 1 Deformations of fiber buckling

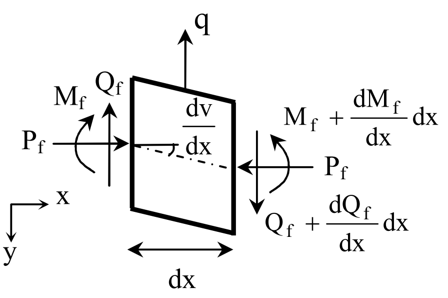

Fig. 3 Free-body diagram of a fiber segment in matrix

Where d_f is fiber diameter and G_f is shear modulus of fiber.

Bending moment is expressed by Equation (2) or (3) dependent on the fiber deformation shown in Fig. 2(a) or 2(b). Actual deformation of fiber may be superposition of the deformations in Fig. 2(a) or 2(b) dependent on the fiber volume fraction. Therefore, bending moment can be written as following generalized form.

$$M_f = -f_{(V_f)} E_f I_f \frac{d^2(v-v_0)}{dx^2} + (1-f_{(V_f)})\frac{\pi d_f^2}{4}\int G_f \frac{d(v-v_0)}{dx}dx \tag{4}$$

First term indicates moment due to bending and second term due to simple shear. $f_{(Vf)}$ is a function of fiber volume fraction which is in the range of $0 \leq f_{(Vf)} \leq 1$. $f_{(Vf)}=1$ for Fig. 1(a) and $f_{(Vf)} = 0$ for Fig. 1(b).

Lateral force can be expressed using foundation modulus k.

$$q = f_{(V_f)} k(v - v_0) \tag{5}$$

Lateral force may decrease with increase of fiber volume fraction because fibers buckle in coordinate phase each other.

Differential equation of the fiber can be obtained using Equation (1), (4) and (5)

$$f_{(v_f)} E_f I_f \frac{d^4(v-v_0)}{dx^4} - (1-f_{(v_f)})\frac{\pi d_f^2}{4} G_f \frac{d^2(v-v_0)}{dx^2} + P_f \frac{d^2 v}{dx^2} + f_{(v_f)} k(v-v_0) = 0 \tag{6}$$

If no deflection and no bending moment is supposed as a boundary condition, homogeneous solution of Equation (6), i.e. the buckling curve with no fiber misalignment is obtained as follow.

$$v = A \sin\frac{\pi}{L_h} x \tag{7}$$

Where A is amplitude of the buckling curve, L_h is a half wavelength. L_h is expressed as follow.

$$L_h = \sqrt[4]{\frac{E_f I_f \pi^4}{k}} \tag{8}$$

Initial misalignment of the fiber is supposed as same to the buckling curve.

$$v_0 = A_0 \sin\frac{\pi}{L_h} x \tag{9}$$

Buckling stress of the fiber is obtained using equations (6), (7) and (9)

$$\sigma_f = \left[f_{(v_f)} \sqrt{\frac{E_f k}{\pi}} + (1 - f_{(v_f)}) G_f \right] (1 - \frac{A_0}{A}) \tag{10}$$

Maximum deflection angle of the fiber $(\gamma_{xy})_{max}$ is

$$(\gamma_{xy})_{\max} = \left[\frac{d(v-v_0)}{dx} \right]_{\max} = (A - A_0)(\frac{\pi}{L_h}) \tag{11}$$

If shear deformation in Fig. 2(b) is supposed, $(\gamma_{xy})_{max}$ coincides to shear strain of the fiber at node.
Equation (10) is rewritten using Equation (11).

$$\sigma_f = \left[f_{(v_f)}\sqrt{\frac{E_f k}{\pi}} + (1-f_{(v_f)})G_f \right]\left(\frac{(\gamma_{xy})_{\max}}{(\gamma_{xy})_{\max} + A_0(\frac{\pi}{L_h})}\right) \quad (12)$$

Maximum initial misalignment of the fiber ϕ_0 is

$$\tan\phi_0 = (\frac{dv_0}{dx})_{\max} = A_0(\frac{\pi}{L_h}) \quad (13)$$

As a result, buckling stress of the fiber can be obtained using Equation (12) and (13).

$$\sigma_f = \left[f_{(v_f)}\sqrt{\frac{E_f k}{\pi}} + (1-f_{(v_f)})G_f \right]\left(\frac{(\gamma_{xy})_{\max}}{(\gamma_{xy})_{\max} + \tan\phi_0}\right) \quad (14)$$

Equation (14) coincides with kink-band theory when $f_{(Vf)}=0$ [7-10]. Equation (14) shows that buckling stress of the fiber depends on the shear modulus if foundation modulus decreased. The foundation modulus decreased with increase of fiber volume fraction because fiber buckles with coordinate phase each other in kink band failure. On the other hand, foundation modulus cannot be ignored for the model of a single fiber in matrix. Foundation modulus of matrix is derived in the next chapter.

3 Foundation modulus of surrounding matrix

There are some reports on the foundation modulus of surrounding matrix [11-13, 15]. In this study, foundation modulus is derived as a simple form using two-dimensional elasticity.
Let's consider a fiber in matrix (Fig.1). Concentrated load q is applied transversely at the center of the fiber, i.e. origin of the axis in Fig.4. Stress component are expressed as follows [21].

$$\sigma_r = -\frac{(3+\nu_m)}{4\pi}\frac{q\cos\theta}{r} \quad (15)$$

$$\sigma_\theta = \frac{(1-\nu_m)}{4\pi}\frac{q\cos\theta}{r} \quad (16)$$

$$\tau_{r\theta} = \frac{(1-\nu_m)}{4\pi}\frac{q\sin\theta}{r} \quad (17)$$

Where ν_m is a Poisson's ratio of matrix.
Corresponding strain components are

$$\varepsilon_r = \frac{\partial v_r}{\partial r} = \frac{\sigma_r - \nu_m\sigma_\theta}{E_m} = -\frac{(3+2\nu_m-\nu_m^2)}{4\pi E_m}\frac{q\cos\theta}{r} \quad (18)$$

$$\varepsilon_\theta = \frac{v_r}{r} + \frac{\partial w_\theta}{r\partial\theta} = \frac{-\nu_m\sigma_r + \sigma_\theta}{E_m} = \frac{(1+2\nu_m+\nu_m^2)}{4\pi E_m}\frac{q\cos\theta}{r} \quad (19)$$

$$\gamma_{r\theta} = \frac{\partial v_r}{r\partial\theta} + \frac{\partial w_\theta}{\partial r} - \frac{w_\theta}{r} = \frac{\tau_{r\theta}}{G_m} = \frac{(1-\nu_m)^2}{2\pi E_m}\frac{q\sin\theta}{r} \quad (20)$$

Where E_m and G_m is Young's modulus and shear modulus of matrix, v_r, w_θ is r and θ-directional displacement. v_r, w_θ is expressed using Equation (18), (19) and (20)

$$v_r = -\frac{(3+2\nu_m-\nu_m^2)}{4\pi E_m}q\cos\theta\ln r + B_1\sin\theta + B_2\cos\theta \quad (21)$$

$$w_\theta = \frac{(1+2\nu_m+\nu_m^2)}{4\pi E_m}q\sin\theta + \frac{(3+2\nu_m-\nu_m^2)}{4\pi E_m}q\sin\theta\ln r + B_1\cos\theta - B_2\sin\theta + B_3 r \quad (22)$$

in which B_1, B_2, B_3 are constants of integration, which are determined from the boundary conditions. Substituting $w_\theta=0$ at $\theta=0$, $B_1=B_3=0$ can be obtained. Y-directional displacement along the y-axis is

$$(v_r)_{\theta=0} = -\frac{(3+2\nu_m-\nu_m^2)}{4\pi E_m}q\ln r + B_2 \quad (23)$$

If y-directional displacement is assumed zero on the y-axis at a distance d_e from the origin (Fig.4) B_2 can be obtained. As a results displacement v_r and w_θ is expressed as follows.

$$v_r = \frac{(3+2\nu_m-\nu_m^2)}{4\pi E_m}q\cos\theta\ln\frac{d_e}{r} \quad (24)$$

$$w_\theta = \frac{(1+2\nu_m+\nu_m^2)}{4\pi E_m}q\sin\theta + \frac{(3+2\nu_m-\nu_m^2)}{4\pi E_m}q\sin\theta\ln\frac{r}{d_e} \quad (25)$$

The relationship between load q and y-directional displacement $(v_r)_{\theta=0}$ is obtained using Equation (24) replacing $\theta=0$ and $r=d_f/2$. Foundation modulus k is

$$k = \frac{4\pi E_m}{(3+2\nu_m-\nu_m^2)\ln\dfrac{d_e}{d_f/2}} \quad (26)$$

Equation (26) indicates that foundation modulus depend not only on matrix property but also fiber diameter.
The foundation modulus increases with increase of fiber deflection. It is also difficult to find distance d_e theoretically. In this study, linear elastic foundation is supposed whose summation of y-directional displacement is equivalent to the original nonlinear elastic foundation. Then foundation modulus k is replaced by an equivalent foundation modulus.
Integral of y-directional displacement from the origin to distance d_e is

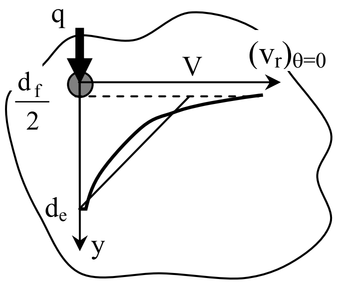

Fig. 4 y-directional displacement along θ=0º

$$S = \int_0^{de} (v_r)_{\theta=0}\, dr = \frac{(3+2\nu_m - \nu_m{}^2)d_e}{4\pi E_m} q \quad (27)$$

A linear spring of constant modulus k_e and length d_e is supposed. Maximum displacement V which is equivalent to integral quantity S is

$$V = \frac{2S}{d_e} \quad (28)$$

Equivalent foundation modulus is expressed as

$$k_{eq} = \frac{q}{V} = \frac{q}{2S/d_e} = \frac{2\pi E_m}{3+2\nu_m - \nu_m{}^2} \quad (29)$$

Equivalent foundation modulus shows larger value in the beginning of fiber deflection and smaller value in the later stage than the actual modulus because actual foundation modulus increase with increase of fiber deflection.

4 Buckling stress of a fiber considering the bending moment

Buckling stress of a fiber in matrix is obtained by Equation (14) and (29).

$$\sigma_f = \left[f_{(V_f)} \sqrt{\frac{E_f k_{eq}}{\pi}} + (1 - f_{(V_f)}) G_f \right] \left(\frac{(\gamma_{xy})_{\max}}{(\gamma_{xy})_{\max} + \tan\phi_0} \right) \quad (30)$$

Equation (30) shows average stress of fiber. Since fiber has initial misalignment bending moment increases with increase of deflection and normal stress due to the bending developed in the fiber. Therefore, fiber may break at the surface at which maximum compressive stress is developed due to the axial stress and bending stress.

Maximum bending moment is developed at antinode of buckling curve. For the bending deformation mode of Fig. 2(a), maximum bending stress $(\sigma_{fb})_{\max}$ at fiber surface is

$$(\sigma_{fb})_{\max} = \frac{M_{\max}}{I_f} \frac{d_f}{2} = \sqrt[4]{\frac{4E_f{}^3 k_{eq}}{\pi}} (\gamma_{xy})_{\max} \quad (31)$$

On the other hand, if shear deformation is supposed in Fig. 2(b) bending stress does not developed.

As discussed above, since fiber deformation is superposition of the two pattern in Fig. 2(a) and 2(b) dependent on the fiber volume fraction maximum compressive stress of fiber $(\sigma_f)_{\max}$ can be expressed as follow.

$$\begin{aligned}(\sigma_f)_{\max} &= \sigma_f + (\sigma_b)_{\max} \\ &= \left[f_{(V_f)} \sqrt{\frac{E_f k_{eq}}{\pi}} + (1 - f_{(V_f)}) G_f \right] \left(\frac{(\gamma_{xy})_{\max}}{(\gamma_{xy})_{\max} + \tan\phi_0} \right) \\ &\quad + f_{(V_f)} \sqrt[4]{\frac{4E_f{}^3 k_{eq}}{\pi}} (\gamma_{xy})_{\max} \end{aligned} \quad (32)$$

Fiber fracture occurs at the surface when compressive stress reached to its compressive strength.

Equation (32) is valid within elastic limit of the matrix. If the matrix yields prior to the fiber failure matrix cannot support fiber sufficiently and unstable fiber deformation is developed which also result in the fiber fracture. In this study, two processes of ultimate fiber failure were considered. First one is a compressive fracture at fiber surface due to compression and bending. Second one is a matrix-yielding initiated unstable fiber deformation.

Matrix is supposed as an elastic-perfectly plastic material. Von Mises yield criterion is used to determine yielding of the matrix.

$$\begin{aligned} Y^2 = \frac{1}{2}[(\sigma_x - \sigma_y)^2 + (\sigma_y - \sigma_z)^2 + (\sigma_z - \sigma_x)^2 \\ + 6(\tau_{xy}^2 + \tau_{yz}^2 + \tau_{zx}^2)] \end{aligned} \quad (33)$$

$$\sigma_x = \frac{\sigma_f}{E_f} E_m \quad (34)$$

$$\sigma_y = -\frac{(3+\nu_m)}{2\pi} \frac{k_{eq}}{d_f} \frac{L_h}{\pi} (\gamma_{xy})_{\max} \sin\frac{\pi}{L_h} x \quad (35)$$

$$\sigma_z = \frac{(1-\nu_m)}{2\pi} \frac{k_{eq}}{d_f} \frac{L_h}{\pi} (\gamma_{xy})_{\max} \sin\frac{\pi}{L_h} x \quad (36)$$

$$\tau_{xy} = G_m \gamma_{xy} = G_m (\gamma_{xy})_{\max} \cos\frac{\pi}{L_h} x \text{ (for } f_{(Vf)}=1) \quad (37)$$

$$\tau_{yz} = 0 \quad (38)$$

$$\tau_{zx} = 0 \quad (39)$$

5 Compression test of a carbon fiber in epoxy matrix

5.1 Experimental setup

5.1.1 Specimen configuration

Compression test of a fiber in matrix was performed by means of four-point bending test. Fig. 5 shows specimen configuration. Acrylic bar was used as a base of the bending test. Two copper foils were wrapped on the acrylic bar. Carbon fiber (T800S, Toray) was put on the acrylic bar and bonded to copper foils using conductive paste (D-550, Fujikura kasei). Carbon fiber was coated with room temperature curable epoxy resin (105/206, West system). Thickness of the coating was approximately 0.6mm. Scratch was made on the acrylic bar using a cutter knife to prevent debonding of the epoxy matrix from the acrylic bar.

Fiber Young's modulus and strength in tension is E_f=294GPa and σ_{ft}=5880MPa. Fiber diameter is

d_f=5μm. Young's modulus and Poisson's ratio of the epoxy matrix is E_m=3GPa and ν_m =0.34.
Strain gage was attached on the surface of acrylic bar to measure the compressive strain. Strain gage was mounted on the tension side of the acrylic bar not to disturb the deformation of the carbon fiber.

5.1.2 Four-point bending test

Schematic of four-point bending test is shown in Fig. 6. Load was applied from the surface at which carbon fiber was mounted to apply compressive load to the carbon fiber. Loading rate is 0.5mm/min.
Electrical resistance of the carbon fiber was measured during the compression test to recognize initiation of the compressive fracture. Electrical resistance was measured by LCR meter(3522, Hioki).

5.2 Experimental results

5.2.1 Electrical resistance change of a carbon fiber due to compression

Compression test of a carbon fiber in matrix was performed by means of four-point bending test. Fig. 7 shows electrical resistance change ratio $\Delta R/R_0$ of carbon fiber due to compression.
Electrical resistance of the fiber was measured simultaneously in the test. Electrical resistance was decreased with increase of compressive strain and then increased with the initiation of compressive failure. Loading was continued for a while after the increase of electrical resistance to develop the fiber fracture for easy observation. Then specimen was removed from the test fixture and fiber fracture was observed using optical microscope.

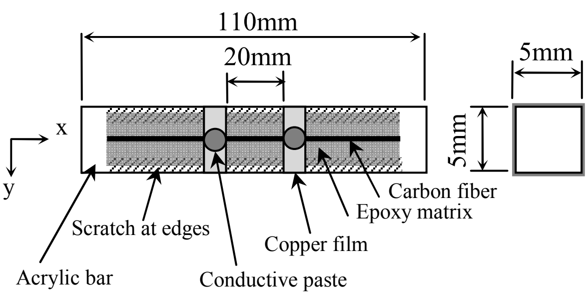

Fig. 5 Specimen configuration

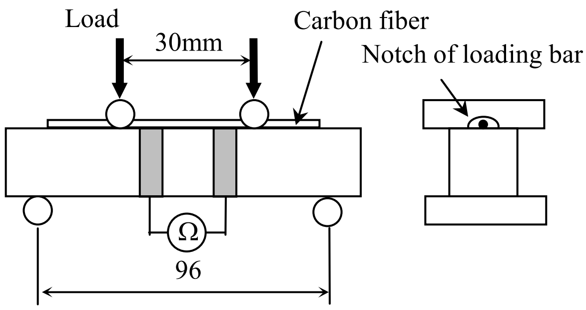

Fig. 6 Schematic of four-point bending test

5.2.2 Buckling wavelength

Fig.8 shows carbon fiber after compression test. Fiber broke at two adjacent locations, which was a result of fiber micro-buckling. This fracture mode is similar to the kink band failure of unidirectional CFRP.
Half wavelength of the micro-buckling is about 35μm which is shorter than kink-band length of unidirectional CFRP [4,7,9,16]. Theoretical buckling half wavelength by Equation (8) is about 20μm. Equivalent foundation modulus shows larger value when fiber deformation is relatively small. Equivalent foundation modulus may overestimate the actual foundation modulus because of small fiber deflection at compressive failure, which will be discussed later.

5.3 Apparent compressive strength of a carbon fiber in matrix

Carbon fiber may show linear elastic until its failure. Compressive strength of carbon fiber σ_{fc} is calculated by Equation (40).

$$\sigma_{fc} = E_f \varepsilon_{fc} \tag{40}$$

Where ε_f is compressive failure strain of carbon fiber. Young's modulus of carbon fiber is supposed as same value both in compression and tension.
Average failure strain of 1.8% was obtained from the experimental results, at which electrical resistance was increased. Since fiber initial misalignment and deflection at failure is small [22, 23] measured failure strain is considered as the average strain of the fiber. Apparent compressive failure of the fiber is calculated as 5387MPa by Equation (40).

5.4 Compressive strength of a carbon fiber in matrix

Since apparent compressive strength was expressed by equation (30) which is not considering the bending stress maximum deflection angle of fiber $(\gamma_{xy})_{max}$ at failure is calculated inversely from equation (30). Then, actual compressive strength of the fiber can be obtained from the equation (32). Figure 9 shows predicted compressive strength of the fiber. Fiber misalignment angle is supposed from ϕ_0=0.1° ~ 1.0°. Dashed-dotted line in the figure indicates apparent compressive strength and broken line indicates tensile strength. Matrix yielding was judged by Equation (33) with Y=70MPa although fiber compressive failure was preceded the matrix yielding.

If fiber misalignment was 0.8° compressive strength of the fiber almost coincides with its tensile strength. It is concluded that compressive strength of the carbon fiber is almost same as the tensile strength. In this case, apparent compressive strength decreased about 500MPa by the bending deformation due to the initial misalignment.

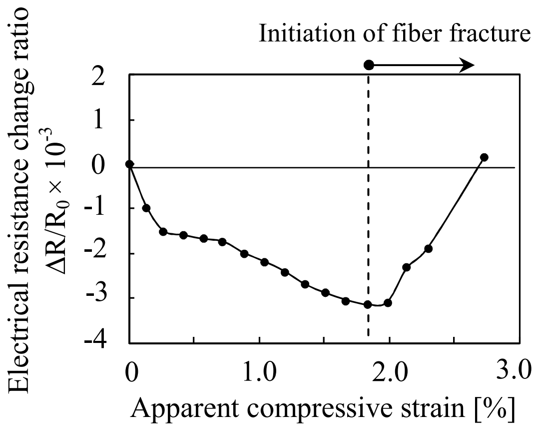

Fig. 7 Electrical resistance change ratio of a carbon fiber in matrix due to compression

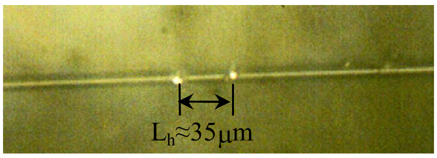

Fig. 8 Buckling of a carbon fiber in epoxy matrix by compression load

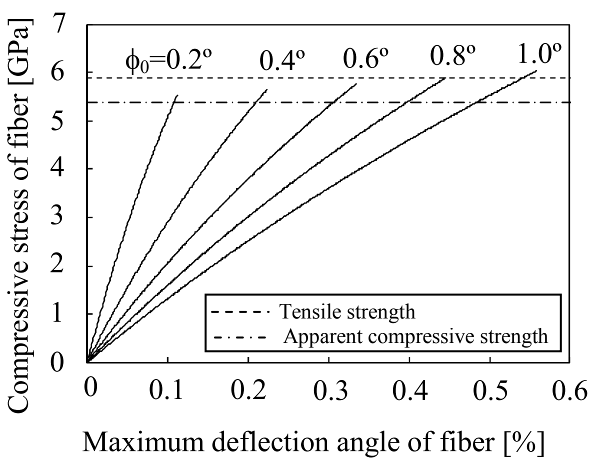

Fig. 9 Prediction of fiber compressive strength

6 Conclusion

Compressive strength of a single carbon fiber in epoxy matrix was investigated. Apparent compressive strength of carbon fiber in matrix was measured by four-point bending test. Actual compressive strength was calculated based on the apparent compressive strength. It is concluded that the fiber compressive strength is almost same to the tensile strength.

References

[1] Toray, TORAYCA T800H data sheet, No.CFA-007,.

[2] Toray, TORAYCA T1000G data sheet, No.CFA-008,.

[3] B. W. Rosen: NASA-CR-60667, 1964.

[4] T. J. Vogler and S. Kyriakides, *Int. J. Solids Struct.*, 38,15, pp 2639-2651, 2001.

[5] R. Gutkin, S. T. Pinho, P. Robinson and P. T. Curtis, *Compos. Sci. Technol.*, 70, 8, pp 1223–1231, 2010.

[6] A. Argon, *Treatise on materials science and technology*, 1, New York: Academic Press, pp 79-114, 1972.

[7] B. Budiansky, *Comput. Struct*, 16, 1, pp 3–12, 1983.

[8] B. Budiansky and N. A. Fleck, *J. Mech. Phys. Solids*, 41, 1, pp 183-211, 1993.

[9] P. M. Jelf and N. A. Fleck, *J. Compos. Mater.*, 26, 18, pp 2706-2726, 1992.

[10] B. Budiansky, N. A. Fleck and J. C. Amazigo, *J. Mech. Phys. Solids*, 46, 9, pp 1637-1653, 1997.

[11] M. A. Sadowsky, S. L. Pu, and M. A. Hussain, *J. Appl. Mech.*, 34, pp 1011-1016, 1967.

[12] L. R. Herrmann, W. E. Mason and S. T. K. Chan, *J. Compos. Mater.*, 1, 3, pp 212-226. 1967.

[13] Y. Lanir and Y. C. B. Fung, *J. Compos. Mater.*, 6, 3, pp 387-401, 1972.

[14] H. T. Hahn and J. G. Williams: NASA TM-85834, 1984.

[15] Y. L. Xu and K. L. Reifsnider, *J. Compos. Mater.*, 27, 6, pp 572-588, 1993.

[16] A. Jumahat, C. Soutis, F. R. Jones, and A. Hodzic, *Compos. Struct.*, 92, 2, pp 295-305, 2010.

[17] H. M. Hawthorne and E. Teghtsoonian, *J. Mater. Sci.*, 10, 1, pp 41-51, 1975.

[18] A. H. Shinohara, T. Sato, F. Saito, T. Tomioka and Y. Arai, *J. Mater. Sci.*, 28, 24, pp 6611-6616, 1993.

[19] M. Nakatani, M. Shioya and J. Yamashita, *Carbon*, 37, 4, pp 601-608, 1999.

[20] M. Shioya and M. Nakatani, *Compos. Sci. Technol.*, 60, 2, pp 219-229, 2000.

[21] S. Timoshenko, Theory of Elasticity (2nd Ed.), McGraw-Hill, New York, 1955.

[22] S. W. Yurgartis, *Compos. Sci. Technol.*, 30, pp 279-293, 1987.

[23] T. Yokozeki, T. Ogasawara and T. Ishikawa, *Compos. Sci. Technol.*, 65, 14, pp 2140-2147, 2005.